JOURNAL OF GEOPHYSICAL RESEARCH, VOL. 102, NO. E4, PAGES 9303–9308, APRIL 25, 1997

Planetary vortices and Jupiter's vertical structure

G. P. Williams

NOAA Geophysical Fluid Dynamics Laboratory, Princeton University, Princeton, New Jersey

Abstract. Measurements of the vertical structure of Jupiter's circulation have recently been made near the equator by the *Galileo* spacecraft probe. In other regions, planetary vortices exist selectively for a limited range of generic (exponential) vertical forms and can be used to probe the atmospheric structure theoretically. A study of vortex genesis with a three-dimensional numerical model produces reasonably realistic simulations of the Great Red Spot for both the generic and galilean forms, provided that Jupiter's winds do not extend much beyond a 500 km depth. However, the actual depth of the winds remains uncertain.

Introduction

Theoretical developments in planetary fluid dynamics, together with high-resolution spacecraft measurements, have led to progress in modeling Jupiter's atmospheric circulation and in defining the physical system. Advances in modeling have been based either on the hypothesis that the motions are confined to a relatively thin upper layer and are driven by the baroclinicity supplied by the Sun and the planet's interior, or on the hypothesis that the motions are deep, extending to the core of the planet and driven by convection. The thin-layer hypothesis has been examined with standard meteorological models that suggest that quasi-geostrophic turbulence theory provides a viable explanation of the multiple jets and ubiquitous eddies, while shallow-water coherence theory underlies the understanding of the major vortices, namely, the Great Red Spot (GRS) and Large Ovals; see the reviews by *Williams* [1985], *Ingersoll* [1990], *Gierasch and Conrath* [1993], *Marcus* [1993], *Rhines* [1994], and *Dowling* [1995]. The deep-envelope hypothesis has been examined with astrophysical models but lies beyond the scope of this paper; see *Busse* [1994], *Manneville and Olson* [1996], *Zhang and Schubert* [1996] for recent appraisals.

All theories have been hampered by the absence, until recently, of observations of the vertical wind structure, although the horizontal form of the circulation is well known at cloud level [*Limaye*, 1986; *Rogers*, 1995]. However, measurements just made by the *Galileo* spacecraft probe may have altered this situation [*Atkinson et al.*, 1996]. Essentially, the probe provides a velocity sample, derived from Doppler measurements at a latitude of $\phi = 6.5°$N, which shows that the winds first increase with depth and then decrease slightly near the 100-km level, as in Figure 1. This profound measurement, remarkable though it may be, has several limitations, the main one being that it comes from a complex tropical regime which, like its terrestrial counterpart, may differ completely from the flow regime in higher latitudes, where the major vortices occur. The *Galileo* orbiter measurements of the GRS, presently under analysis, should reveal the wind structure of midlatitudinal flows and thereby indicate how globally relevant the probe measurements, presently under reanalysis, are, provided the vertical extent covered by both is great enough to be definitive.

Paper number 97JE00520.

Recent studies with a three-dimensional numerical model seek to address these structural issues by experimenting with various hypothetical forms to find those that favor vortex stability and genesis [*Williams*, 1996]. Exponential forms seem to provide the simplest relevant solutions. The vortex modes for such generic structures can also be extended to comply with the galilean form without losing their essential characteristics. For relatively thin atmospheres overlying a deep abyss, single vortex states resembling the GRS can be generated by a baroclinically unstable easterly jet for both the generic and galilean structures but with differing degrees of generality. The solutions presented here extend those reported earlier to consider greater depths and larger velocities and lead to more realistic GRS simulations.

Three-Dimensional Model

Our calculations use the time-dependent, three-dimensional primitive equations of motion with a Boussinesq equation of state, solved for a regional channel in the southern hemisphere by finite difference methods; see *Williams* [1996] for details. The resolution is set to 1° in latitude, 2° in longitude, and 20 levels in the vertical, with an exponential distribution placing most gridpoints aloft in the active layer. The Jovian parameters are a = 71,400 km, $\Omega = 1.76 \times 10^{-4}$ s^{-1}, $g = 26$ m s^{-1}, H = 15,000 km, and $\alpha = 0.005$ K^{-1} for the planetary radius, rotation rate, gravity, fluid depth, and Boussinesq coefficient. Although applying this process model to depths as extensive as the gas-liquid transition at 1000 km or the liquid-metallic interface at 15,000 km exceeds the formal validity of the equations, the solutions are still relevant, provided the main motions are confined to a thin upper layer [cf. *Williams and Robinson*, 1973]. Nonetheless, we do expect distortions in the vertical variations, and these could account for some of the inadequacies of the solutions.

We present two comparative solutions: cases G1 and G2, for the generic and galilean jet structures, respectively, shown in Figure 1. For the G1 case, the generic sech (Nz') form with $N = 200$ is chosen, although the exp (Nz') form would do equally as well. The G2 profile matches the probe data aloft, where it defines a mixed layer of depth $d = 100$ km and then decays exponentially to a depth $h = 500$ km, which effectively defines the extent of the active layer. The G2 "galilean" form (our terminology is purely for convenience) is represented by the function sech $[N(z' - d')]$ with $N = 130$, where z' =

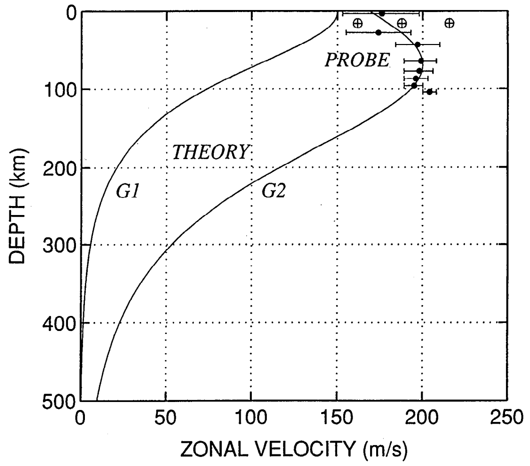

Figure 1. Zonal wind profiles comparing the flow measured by the *Galileo* spacecraft probe (solid dots and error bars) [*Atkinson et al.*, 1996] with the generic (G1) and galilean (G2) theoretical forms. The G1 profile is plotted with an arbitrary amplitude. Crosses mark the values of the angular-momentum conserving wind, $u_m = a\Omega \sin^2 \phi/\cos \phi$, associated with the axisymmetric regime, evaluated at the three latitudes $\phi = 7° \pm 0.5°$.

z/H and $d' = d/H = -0.6$ denote the nondimensional vertical coordinate and mixed layer depth, and N defines the confinement rate. In addition, background temperature fields are set at 3.5 $\int (\text{sech}\, Nz')dz$ and at 2.4 $\int [\text{sech}\, N(z' - d')]dz$ for G1 and G2, respectively, so that the static stability has the same structure as the velocity, where the integrals are normalized to unity. These fields are primarily of exponential form and could be established by radiative transfer in an opaque atmosphere. They produce Brunt-Vaïsälä stability parameters of about 5×10^{-6} s^{-2} and Rossby deformation radii of about 1500 km.

The galilean G2 form is chosen to represent the maximum complexity inherent in the data yet remain compatible with basic vortex theory. Introducing a reversed shear and baroclinicity in the mixed layer activates the second baroclinic mode and vertical interactions that modify processes dominated by the first baroclinic mode. The simpler case which minimizes the complexity in the data and assumes a uniform flow can be dealt with by flattening a generic form aloft, as in Figures 39–41 of *Williams* [1996]. The main hypothesis underlying the G2 form, namely, that the winds decay exponentially over a depth of 400 km, is tested by the calculations and involves far less extrapolation than assuming the winds remain constant down to the planet's core.

In both calculations, geostrophically balanced zonal jets are inserted initially and allowed to evolve to examine how the above structures influence the generation of vortices by the main unstable easterly current. The alternating westerly and easterly jets have amplitudes that decrease poleward and have patched sinusoidal profiles that vanish at fixed latitudes, given by (200, −100, 60, −20) m s^{-1} and −(10, 19, 28, 40)° for G1, and by (320, −100, 60, −20) m s^{-1} and −(0, 11, 19, 28, 40)° for G2. The two cases differ only near the equator: the G1 flow is set constant at 200 m s^{-1} over $\phi = 0°$ to $-7°$, whereas the G2 flow peaks at $\phi = -5.5°$ and vanishes at $\phi = 0°$, although it soon goes unstable and creates a 220 m s^{-1} superrotation at the equator (cf. Figure 3).

Generic Vortices

Calculations over a wide range of conditions reveal that generic vortex stability (i.e., coherence and persistence) depends primarily on $\delta = h/H$, the thickness of the active layer relative to the abyss, and on the size of the storm relative to the Rossby deformation scale [*Williams*, 1996]. In particular, large anticyclones with a large thickness ratio of $\delta \sim 1/5$ remain coherent but tend to migrate toward the equator, where they disperse rapidly. Thinner vortices with $\delta \sim 1/10$ migrate more slowly, however, and can be stabilized by the blocking action of weak easterly jets. Even thinner vortices with $\delta \sim 1/20$ are absolutely stable, remaining coherent indefinitely and not migrating at all, just propagating steadily westward. Such vortices can exist freely or can coexist with stable alternating jets of the same structure. On the other hand, barotropic jets destroy baroclinic vortices, and barotropic vortices decay rapidly, thus excluding deep flow structures.

When zonal currents are confined to thin atmospheres with $\delta \leq 1/20$, the easterly jets develop baroclinic instabilities that take on the form of solitary waves rather than the usual periodic waves seen in thick atmospheres with $\delta \geq 1/5$. The solitary (nonlinear long Rossby) waves grow into vortices that exhibit a variety of configurations and evolutionary paths. Most cases result, after a series of mergers and enough time, in a single vortex state. Single vortex states can also arise at the start and persist thereafter, but they occur over a narrower parameter range. Exceptions to the merging tendency do occur, with multivortex states persisting when the merger timescale is too long to be realized or when the vortices are too alike to approach one other. Single vortex states resembling all phases of the GRS, with sizes ranging from 15° to 50° in longitude and with temperature gradients, velocities, propagation rates, and oscillations in the observed range, can be generated either ab initio or by mergers.

Comparative Vortex Genesis

Theoretically, the generic modes can exist for a wide range of values for the vertical scales h and H, provided that their relative ratio δ remains small. Thus solutions with $h \sim 50$ km and $H \sim 1500$ km are identical in form to those with $h \sim 500$ km and $H \sim 15{,}000$ km if the temperatures are reduced accordingly by a factor of 10 to maintain similar velocities. The equations, however, become less valid for the deeper fluids. The absence of a definitive vertical scale limits the quantitative application of the general vortex theory to Jupiter at present. Flows with the galilean structure, however, are constrained specifically to the scales seen in Figure 1 but otherwise behave in almost the same way as the generic modes, provided that the upper mixed layer remains reasonably thin. In particular, vortices remain coherent and persistent if $d \leq h/5$ and $h \leq H/20$.

To illustrate these results, we present two comparative solutions for vortex genesis in the generic and galilean systems that exhibit both the ab initio and merger path types, in Figures 2–5 and Plate 1. (In the figures the temperature field excludes the static component, and the dashed lines denote negative values.) The single and double vortex states that arise initially do so generally when the jets are very strong and the static stability is minimal. In the generic G1 case in Figure 2, a single large anticyclone grows from a wave packet perturbation of an unstable easterly jet through the development of a sharp three-dimensional frontal surface that propagates westward and eventually occludes. Similarly, in the galilean G2 case the ini-

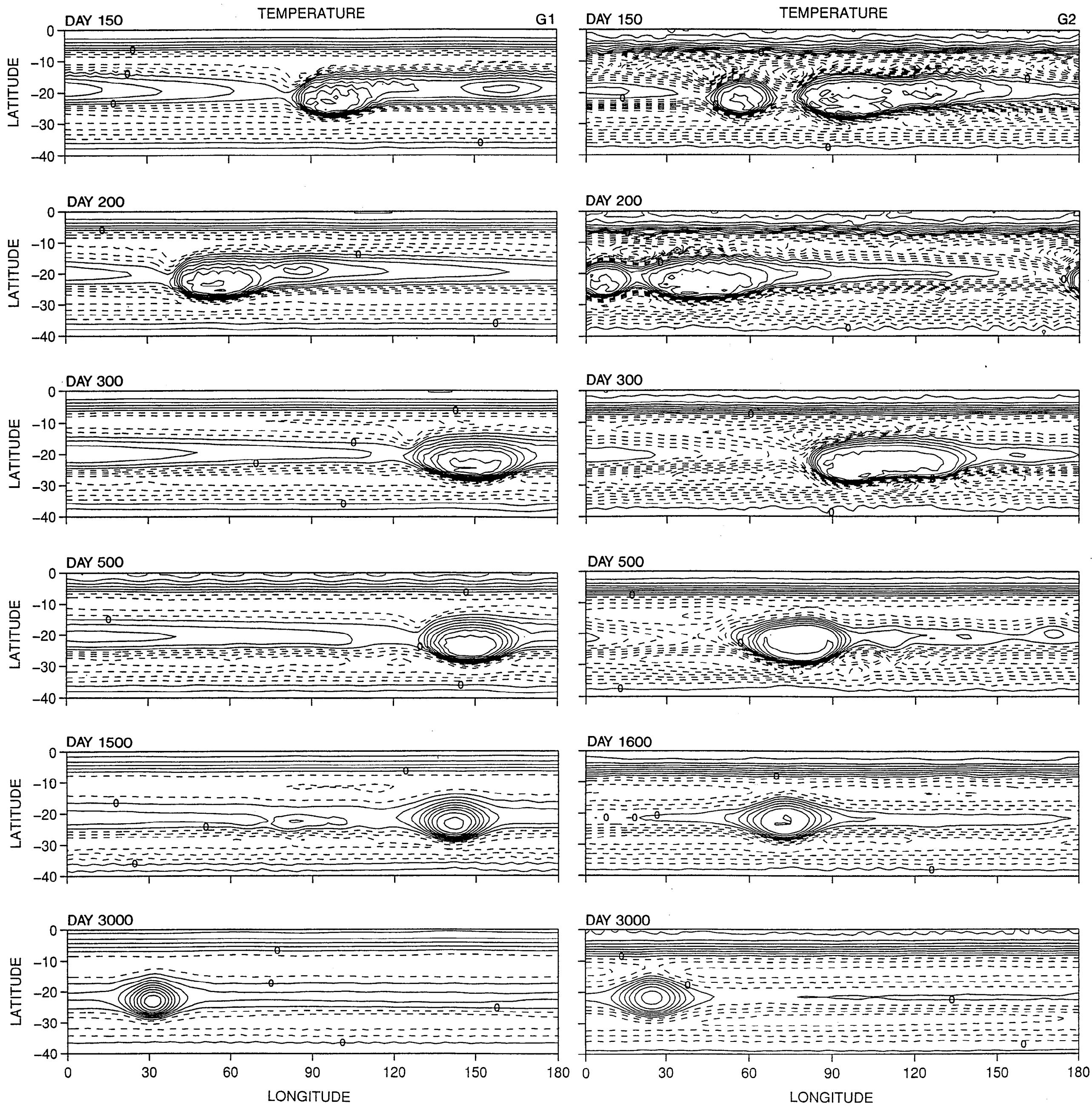

Figure 2. Horizontal temperature sections comparing the generation of single long-lived vortices from baroclinically unstable easterly jets, ab initio for the G1 case and by a merger for the G2 case. The sections are taken at depths of (82, 108) km and use contour intervals of (0.3, 0.1) K for the (G1, G2) cases.

tial disturbance splits into two fronts that grow into two unequal anticyclones that soon merge into one. This behavior is typical of galilean flows and distinguishes them clearly from the generic flows. In both cases the final vortex is fully formed by 500 days but continues to evolve slowly, with only the G2 storm weakening significantly.

The initial vertical structure of the G2 jets is maintained best by the tropical westerly (where it was measured by the probe), even though that current undergoes an instability that creates the equatorial superrotation (Figure 3). Elsewhere, the jets tend to develop a more uniform flow in the mixed layer. The vortices in both systems develop and maintain the same vertical form and extent as their generating jets (Figure 4). Although the G2 storm displays a large and distinct isothermal core in the horizontal sections at 500 days in Figure 2, we see from Figure 4 that it does so only for a limited range of depths around 100 km. At such depths, the strongest flows occur in a horizontal ring at the periphery of a quiescent center, as is observed both in the ocean [*Olson*, 1991] and in the Voyager data [*Mitchell et al.*, 1981; *Sada et al.*, 1996]. Finally, we note from the three-dimensional isothermal surface in Plate 1 that at the end of the formation phase the vortex remains connected to the warm easterly jet near the tropopause and has a distinctly asymmetric keel shape.

The asymmetry of the vortices (they are significantly stronger on the poleward side in Figure 3 and Plate 1) diminishes

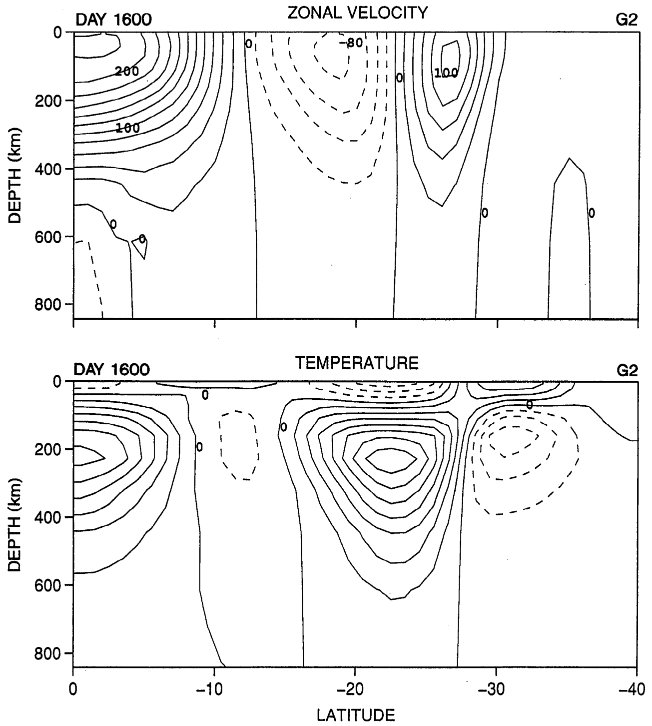

Figure 3. Meridional sections for the G2 case showing the local zonal velocity and temperature at the longitude, 73°, of the vortex center, with contour intervals of 20 m s^{-1} and 0.2 K, over an upper level subdomain.

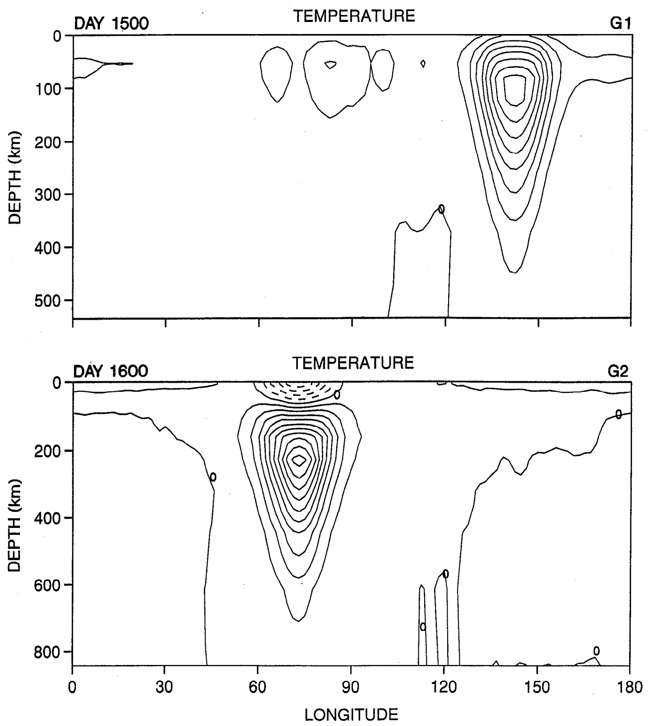

Figure 4. Vertical sections comparing the temperature structures for the G1 and G2 vortices through their centers, at latitudes −24° and −23°, with contour intervals of 0.3 and 0.15 K, respectively, over an upper level subdomain.

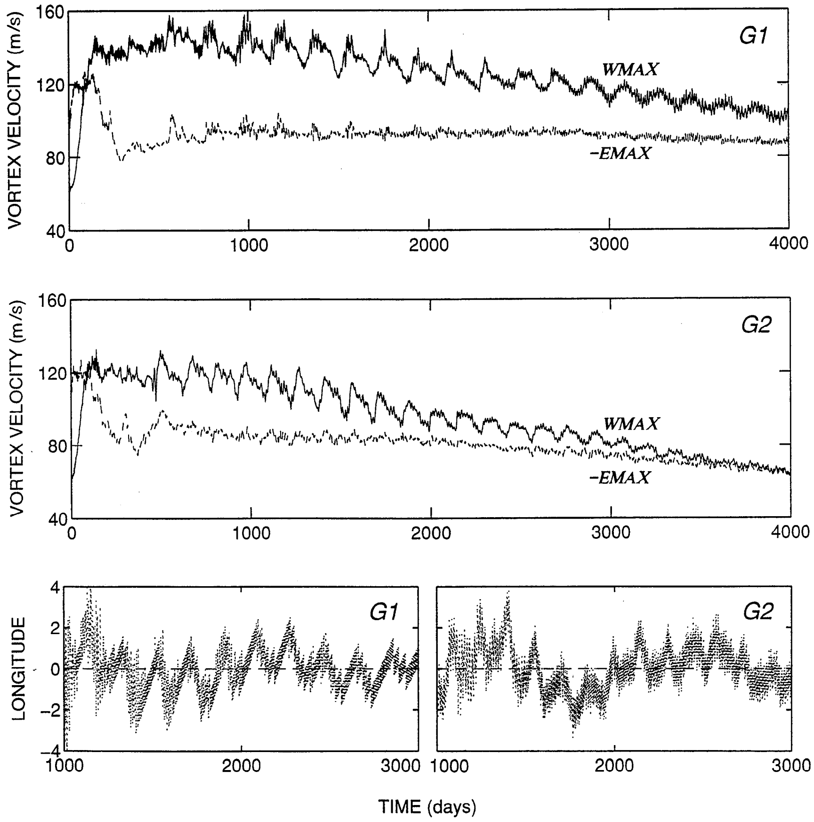

Figure 5. (top and middle) Evolution of the asymmetry and oscillation in the maximum westerly and easterly winds in the vortex zones. (bottom) Oscillation in the deviations of the longitudinal position of each vortex from its quasi-linear progression over 3673° (G1) and 4704° (G2) of longitude during 4000 days. All variables are sampled at 1-day intervals.

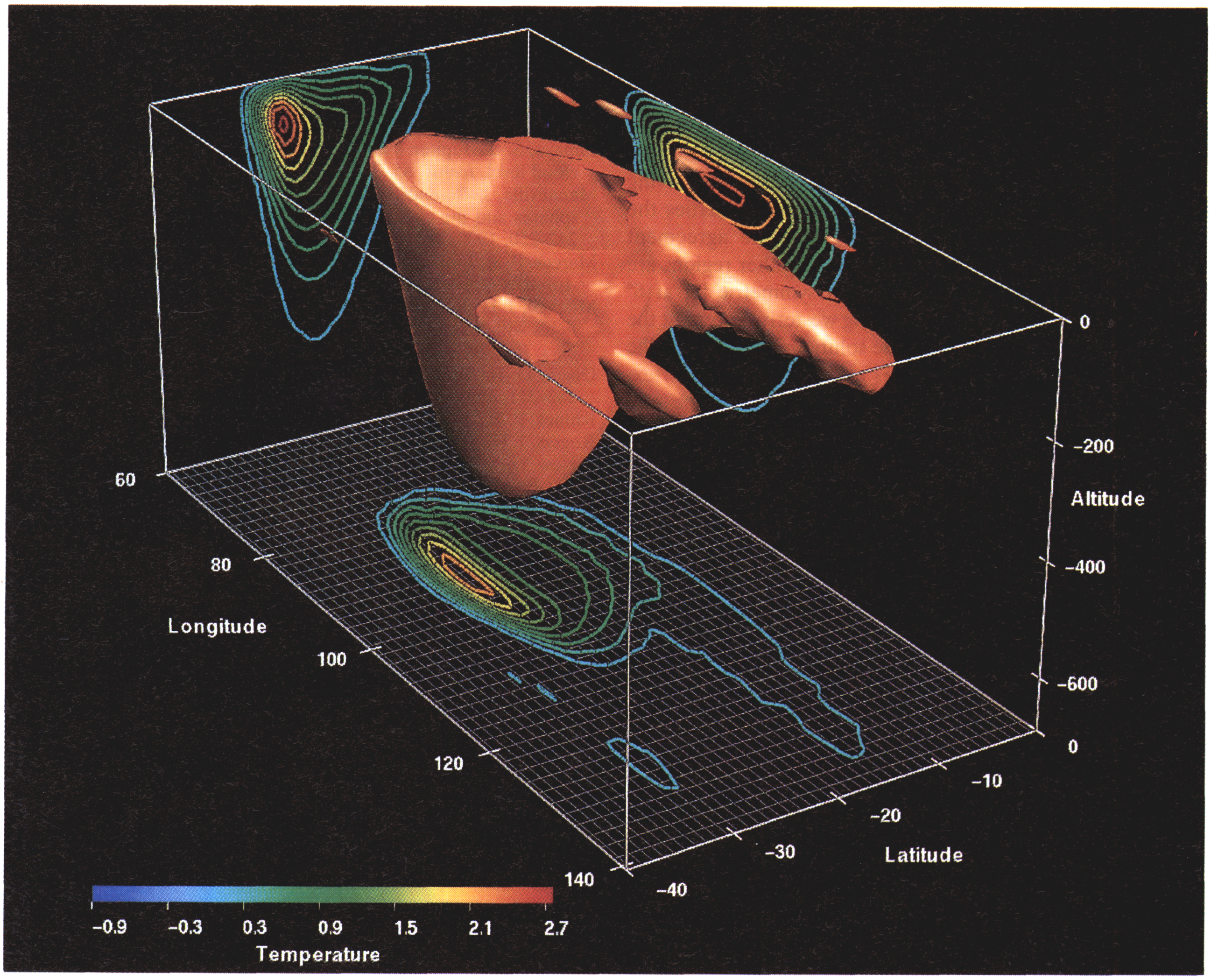

Plate 1. Three-dimensional configuration of the G1 vortex at 550 days defined by an outer isothermal surface of 0.08 K, and by sections taken through the center and top and projected onto the axes, with a contour interval of 0.25 K.

with time according to the relative values of the maximum westerly and easterly velocities shown in Figure 5. In the G1 case, however, only the westerly component decreases and does so until it matches the steady easterly component and both equilibrate. However, in the G2 case both components continue to decrease through the action of the second baroclinic mode. This suggests that generic storms are more likely to survive indefinitely than the galilean type. The maximum velocity levels, 150 m s^{-1} and 120 m s^{-1}, reached by the G1 and G2 vortices compare well with the GRS levels and are determined primarily by the strength of the generating easterly jets. The G1 and G2 vortices, however, propagate westward at phase speeds of 12 and 16 m s^{-1}, respectively, which are higher than the observed.

The velocity maxima in Figure 5 also exhibit well-organized oscillations with periods of about 190 days for G1 and 150 days for G2. They are caused by recurring interactions between the vortex and the wave disturbance it induces in the neighboring westerly jet at $\phi = -25°$, but they decrease in amplitude as the vortex becomes more symmetric. As is appropriate for wave phenomena, the ratio of the oscillation periods for the two cases varies inversely as the ratio of the westward phase speeds of the vortices, with both equaling 1.3. Furthermore, the longitudinal position of each vortex also fluctuates about the mean drift, with a 2° amplitude and with the same period and phase as the associated velocity oscillations. These well-defined variations may be related to the 90-day and 1° amplitude oscillation seen in the longitudinal position of the GRS [*Solberg*, 1969; *Rogers*, 1995].

Planetary Implications

Overall, the genesis and persistence of stable vortices with realistic scales, speeds, and oscillations in the solutions support the idea that Jupiter's atmospheric motions are confined to a thin layer overlying a deep abyss. Vortices with generic exponential structures are significantly more persistent and, being rescalable in the vertical, can exist for a greater range of depths, from 50 to 500 km. Those with the galilean structure and its 100 km mixed layer are, however, limited to an active layer of 500 km above an inactive abyss of 15,000 km. The *Galileo* orbiter data may reveal a GRS structure that lies somewhere between these two extremes. Vortex theory clearly provides a way of examining the vertical structure of the Jovian circulations but needs further development if it is to yield the preferred scales, not just the preferred forms.

From the vortex point of view, the flow structure observed at 6.5° latitude could represent the global state, but this seems unlikely, given the diversity of the regimes. Indeed, the agreement in Figure 1 between the observed wind speeds and the velocities associated with an angular-momentum conserving flow suggests that an axially symmetric regime underlies the low-latitude system [*Held and Hou*, 1980] (the agreement seems too close to be coincidental), whereas other regions are clearly turbulent. Instabilities in such a symmetric jet at 6° latitude readily produce a superrotating westerly current at the equator, as is shown in Figure 3. The solutions also support the hypothesis that close dynamical ties exist between the vortex-bearing atmospheres of Jupiter, Saturn, and Neptune and Earth's oceans. If we regard the ocean as being essentially a system with a structure of the order of exp $(10z')$, then Jupiter may be regarded as a primeval or primitive ocean of the order of exp $(100z')$.

Acknowledgments. I am greatly indebted to Syukuro Manabe for the support that made this study possible. Thanks also go to Ron Pacanowski and John Sheldon for assistance with the three-dimensional graphics, to Wendy Marshall for typing, to Catherine Raphael for drafting, and to the reviewers for their perceptive comments.

References

Atkinson, D. H., J. B. Pollack, and A. Seiff, Galileo Doppler measurements of the deep zonal winds at Jupiter, *Science*, *272*, 842–843, 1996.

Busse, F. H., Convection driven zonal flows and vortices in the major planets, *Chaos*, *4*, 123–134, 1994.

Dowling, T. E., Dynamics of Jovian atmospheres, *Annu. Rev. Fluid Mech.*, *27*, 293–334, 1995.

Gierasch, P. J., and B. J. Conrath, Dynamics of the atmospheres of the outer planets: Post-Voyager measurement objectives, *J. Geophys. Res.*, *98*, 5459–5469, 1993.

Held, I. M., and A. Y. Hou, Nonlinear axially symmetric circulations in a nearly inviscid atmosphere, *J. Atmos. Sci.*, *37*, 515–533, 1980.

Ingersoll, A. P., Atmospheric dynamics of the outer planets, *Science*, *248*, 308–315, 1990.

Limaye, S. S., Jupiter: New estimates of the mean zonal flow at the cloud level, *Icarus*, *65*, 335–352, 1986.

Manneville, J. B., and P. Olson, Banded convection in rotating fluid spheres and the circulation of the Jovian atmosphere, *Icarus*, *122*, 242–250, 1996.

Marcus, P. S., Jupiter's Great Red Spot and other vortices, *Annu. Rev. Astron. Astrophys.*, *31*, 523–573, 1993.

Mitchell, J. L., R. F. Beebe, A. P. Ingersoll, and G. W. Garneau, Flow fields within Jupiter's Great Red Spot and White Oval BC, *J. Geophys. Res.*, *86*, 8751–8757, 1981.

Olson, D. B., Rings in the ocean, *Annu. Rev. Earth Planet. Sci.*, *19*, 283–311, 1991.

Rhines, P. B., Jets, *Chaos*, *4*, 313–339, 1994.

Rogers, J. H., *The Giant Planet Jupiter*, 418 pp., Cambridge Univ. Press, New York, 1995.

Sada, P. V., R. F. Beebe, and B. J. Conrath, Comparison of the structure and dynamics of Jupiter's Great Red Spot between the Voyager 1 and 2 encounters, *Icarus*, *119*, 311–335, 1996.

Solberg, H. G., A three-month oscillation in the longitude of Jupiter's Red Spot, *Planet. Space Sci.*, *17*, 1573–1580, 1969.

Williams, G. P., Jovian and comparative atmospheric modeling, *Adv. Geophys.*, *28A*, 381–429, 1985.

Williams, G. P., Jovian Dynamics, I, Vortex stability, structure, and genesis, *J. Atmos. Sci.*, *53*, 2685–2734, 1996.

Williams, G. P., and J. B. Robinson, Dynamics of a convectively unstable atmosphere: Jupiter?, *J. Atmos. Sci.*, *30*, 684–717, 1973.

Zhang, K., and G. Schubert, Penetrative convection and zonal flow on Jupiter, *Science*, *273*, 941–943, 1996.

G. P. Williams, NOAA Geophysical Fluid Dynamics Laboratory, Princeton University, Forrestal Campus, U.S. Route 1, P.O. Box 308, Princeton, NJ 08542. (e-mail: gw@gfdl.gov)

(Received November 8, 1996; revised February 14, 1997; accepted February 18, 1997.)